JOURNAL OF GEOPHYSICAL RESEARCH, VOL. 105, NO. A6, PAGES 12,895–12,906, JUNE 1, 2000

Time-dependent transport of field-aligned bursts of electrons in flickering aurora

L. Peticolas and D. Lummerzheim
Geophysical Institute, University of Alaska Fairbanks

Abstract. We have developed a time-dependent auroral electron transport model to study emission rates caused by field-aligned bursts of electrons (FABs) seen in flickering aurora. We simulate flickering FABs by turning on and off a downward electron intensity distribution at a given frequency. We assume this electron beam originates and is modulated at an altitude of 4000 km. We apply collisionless transport from 4000 to 600 km and solve a time-dependent Boltzmann equation below 600 km. Because FABs have significant flux over a large energy range, dispersion has the most important effect on the resulting emission rates. We find that for a 5 Hz flickering FAB, the column emission rate varies 93% from peak to valley, whereas for 100 Hz flickering, the variation in column emission rate is only 12% from peak to valley. This variation is dependent on the frequency and source altitude. We show that with a time-dependent transport calculation and a filtered fast photometer or imager looking in the zenith, it is possible to obtain an upper limit on the altitude from which the optical flickering originates. We also study what electron detectors on a rocket or satellite might measure in the lower ionosphere when there exists field-aligned bursts of electrons. Velocity dispersion calculations will give source altitudes much lower than is correct if they are derived from low energy electrons (<2 keV) measured at altitudes below 150 km. Our results agree with the interpretation that field-aligned bursts are a temporal rather than spatial feature, and from this knowledge it should be possible to reconstruct the initial electron distribution function at the source altitude.

1. Introduction

Optical instruments are important in providing spatial, temporal, and spectral information about the aurora as well as information regarding the upper atmosphere during an auroral display. Most optical aurora are the consequence of electrons colliding with the upper atmosphere, leaving neutrals and ions in vibrationally and electronically excited states, thus producing altitude dependent optical emissions and ionization. Studying the energy deposition of auroral electrons in order to obtain emission and ionization rates can be important in analyzing optical data as well as learning how precipitating electron fluxes are modified by the upper atmosphere.

The theory of electron energy deposition is studied by solving the transport of a given downward electron flux in the lower ionosphere as a function of energy, altitude, and pitch angle. The transport equation for auroral electrons has been solved using various techniques. For emission and ionization rates of near isotropic electron spectra, it is sufficient to solve the transport equation using a two-stream approximation [*Banks and Nagy*, 1974]. However, for electron intensities that are anisotropic it can be important to have a higher pitch angle resolution. Multistream solutions have been obtained by solving the transport equation using the discrete-ordinate method [*Stamnes*, 1981; *Lummerzheim and Lilensten*, 1994], by solving the equation as an eigenvalue problem [*Strickland et al.*, 1989], and by solving the equation using a Monte-Carlo numerical technique [*Solomon*, 1993]. All of the solutions to the auroral electron transport equation are steady state solutions since for most studies which use such calculations the electrons which create the aurora move much more rapidly than the auroral forms. However, there are aurora in which the primary auroral electrons and the secondaries produced in collisions do not reach a steady state before the incident particle flux changes, such as in flickering aurora. Such aurora requires a time-dependent electron calculation to correctly determine the time sequence of emission and ionization rates.

When viewed in the zenith, flickering aurora is a type of auroral display in which spots of optical intensity within a discrete arc modulate in brightness at frequen-

Paper number 1999JA000398.
0148-0227/00/1999JA000398$09.00

cies from 2-20 Hz [*Beach et al.*, 1968; *Berkey et al.*, 1980; *McFadden et al.*, 1987] to over 100 Hz [*McHarg et al.*, 1998]. These spots are typically 1-5 km in diameter and flicker coherently for seconds. When viewed at an angle to the discrete arc, the flickering elements are vibrating columns of optical intensity [*Kunitake and Oguti*, 1984]. Flickering is observed in bright, active aurora such as in auroral surges [*Berkey et al.*, 1980].

In situ periodic fluctuations in measurements of electron differential flux were recorded as early as 1966 [*Evans*, 1967]. These measurements showed periodicities around 10 Hz in 1-120 keV electrons at altitudes around 90-200 km. The fluctuations were strongest for electrons greater than 60 keV. Similar results were deduced from measurements of particles with energies greater than 85 keV at similar altitudes [*Arnoldy*, 1970; *Spiger and Anderson*, 1985]. Since then, rocket and satellites have recorded periodic fluctuations from a few hertz to near 100 Hz in lower energy electron detectors and at altitudes greater than 250 km [*Lin and Hoffman*, 1979; *Arnoldy et al.*, 1985; *McFadden et al.*, 1987]. From these studies, the fluctuations have been measured as strongly field aligned and have thus been given the name field-aligned bursts (FABs). Pitch angle dispersion has been measured more recently [*Temerin et al.*, 1993; *Arnoldy et al.*, 1999] implying that the modulation is not completely in the field-aligned component. Source altitudes for the modulation of the electron fluxes have been calculated from velocity dispersion [*Evans*, 1967; *McFadden et al.*, 1987; *Arnoldy et al.*, 1999], from pitch angle dispersion [*Temerin et al.*, 1993; *Arnoldy et al.*, 1999], from the time lag between precipitating electrons and the associated Alfvén wave [*Lund et al.*, 1995], and by determining the altitude at which the oxygen or hydrogen cyclotron frequency matches the measured electron flux modulation frequency, which assumes that flickering is caused by electromagnetic ion cyclotron waves [*Temerin et al.*, 1986; *Lund et al.*, 1995]. Such calculations have provided a large range of source altitudes from 1300 [*Evans*, 1967] to 8000 km [*McFadden et al.*, 1987]. A few of the papers discussing measurements of electron fluctuations also mention simultaneous optical measurements [*Spiger and Anderson*, 1985; *McFadden et al.*, 1987; *Lund et al.*, 1995; *Arnoldy et al.*, 1999]. All of these measurements recorded optical flickering in the discrete arcs traversed by the rocket or satellite measuring the electron modulations.

In this paper, we study the relation between optical emissions and the incident electron flux in flickering aurora. For this purpose we have developed a time-dependent transport simulation. For validation we compare it with a steady state transport model. We then use the model to study the effect of modulated field-aligned bursts on optical emission rates. Finally, we study how the upper atmosphere modifies these field-aligned burst intensities and discuss the implications for flickering aurora. The term "intensity" in electron transport studies refers to the number of electrons passing through a unit surface and unit solid angle per energy and time. In this paper, this term is used synonymously with differential electron flux in rocket and satellite measurements.

2. The Time-Dependent Transport Equation

In our auroral electron transport calculations, we assume that transport perpendicular to the magnetic field line is much smaller than parallel transport, which allows the equation to be solved in one spatial dimension along the field line. Parallel electric fields, the converging magnetic field, and gravity all affect electrons, but the effects of these forces on electrons are small in the region of our simulation box, from 90 to 650 km, and we do not include them. Since there is an azimuthal symmetry in the velocity of the electrons, which follow spirals along magnetic field lines, we can solve the equation in two velocity dimensions: perpendicular, $v_\perp$, and parallel, $v_\parallel$, to the magnetic field. For ease of comparing solutions with rocket and satellite electron measurements, we make a transformation from two-dimensional velocity space, $I(v_\perp, v_\parallel)$ to energy, E, and cosine of the pitch angle, μ, space, $I(E, \mu)$. We also assume that particle-wave interactions are negligible. For steady state solutions to the auroral transport equation, these are the assumptions that are typically made [*Stamnes*, 1981; *Strickland et al.*, 1989; *Solomon*, 1993; *Lummerzheim and Lilensten*, 1994].

We make a few additional simplifications to help compensate for the increase in computer run time that adding the time-dependent term to the transport equation requires. Our first simplification is to assume that the electrons are field aligned, which allows us to solve the equation in one velocity dimension only, $v_\parallel$. The pitch angle dispersion given by *Temerin et al.* [1993] and *Arnoldy et al.* [1999] were both seen in the high energy electrons around the peak inverted V energy. These electrons are assumed to come from the hot plasma sheet and are either modulated below the potential drop by electromagnetic ion cyclotron waves as suggested by *Temerin et al.* [1986, 1993] or are modulated by the potential drop turning on and off as suggested by *Arnoldy et al.* [1999]. The lower energy electrons, which are also observed to fluctuate [*Lin and Hoffman*, 1979; *Arnoldy et al.*, 1985; *McFadden et al.*, 1987], are the FABs, which are strongly field aligned. Even though the plasma sheet electron modulations will be important to the optical signatures in the lower ionosphere, owing to computational constraints, we only model the lower energy FABs from an energy of 3 keV down to 10 eV. Such field-aligned bursts have been measured in the absence of high energy electrons [*Lin and Hoffman*, 1979; *Johnstone and Winningham*, 1982]. Future time-dependent transport models should include pitch angle resolution and high energies in order to include the

modulated high energy, pitch angle dispersed electrons which will certainly add to the ionization and emission rates in the lower ionosphere.

Our second simplification is that we separate the transport of the precipitating electrons from the energy degradation and transport of the secondary electrons. We then assume that the precipitating electrons lose their energy in small increments and thus justify the use of the Continuous Slowing Down (CSD) approximation in the form of an energy derivative of an energy loss function. This CSD approximation is justified for high energy electrons but implies a significant compromise for the energy range below 3 keV [*Strickland et al.*, 1976], our maximum energy. We also do not include scattering of these electrons, but we do include the effect of scattering by a modified energy loss function. The loss function and the CSD approximation is discussed in detail in the comparison of the time-dependent solution with a steady state solution.

For the secondary electrons we make the assumptions that they do not move in space and there is no angular scattering. These assumptions result in an accurate secondary electron flux below 200 km since the high-collision frequencies below this altitude, where most of the secondary electrons are produced, imply that the electrons have a high probability of scattering and losing energy. The large scattering depth justifies neglecting transport in altitude. Thus the secondary electron intensity using the above mentioned assumptions should agree with the electron intensity without these assumptions.

We separate the precipitating electrons and secondary electrons into two equations. The transport of field-aligned precipitating electrons which, with the above assumptions, is now a differential equation instead of an integro-differential equation:

$$\sqrt{\frac{m}{2E}}\frac{\partial I_1(E,z,t)}{\partial t} - \frac{\partial I_1(E,z,t)}{\partial z} = \frac{\partial (I_1(E,z,t)L_{en}(E,z))}{\partial E}, \quad (1)$$

and the second equation describes the production and energy degradation of the secondary, low-energy electrons:

$$\sqrt{\frac{m}{2E}}\frac{\partial I_2(E,z,t)}{\partial t} = -\sum_k n_k(z)\sigma_k^{\rm tot}(E)I_2(E,z,t) + \sum_k n_k(z)\sum_j \int R_k^j(E,E')\sigma_k^{\rm ion}(E')I_2(E',z,t)dE' + \sum_k n_k(z)\int_{2E+W}^{\infty} R_k^s(E,E')\sigma_k^j(E')I_1(E',z,t)dE' + \frac{\partial (I_2(E,z,t)L_{ee}(E,z))}{\partial E}, \quad (2)$$

where $I_1(E,z,t)$ is the high energy electron intensity, $I_2(E,z,t)$ is the low energy electron intensity, E is the kinetic energy of the electrons, z is altitude, t is time, m is the electron mass, $L_{en}(E,z)$ is the energy loss function due to collisions with the neutrals, $L_{ee}(E,z)$ is the loss function due to collisions with the ambient thermal electrons, the summation over k represents the sum over atmospheric neutral species, $n_k(z)$ is the atmospheric density for species k, $\sigma_k^{\rm ion}(E)$ is the electron impact ionization cross section for species k, $\sigma_k^{\rm tot}(E)$ is the total energy loss cross section for species k, $R_k^j(E,E')$ is the energy redistribution function for the jth energy loss process and the kth species. For the redistribution of secondaries, $R_k^s(E,E')$, we use a parameterization based on laboratory measurements [*Opal et al.*, 1971].

We solve the two equations sequentially. Equation (1) is solved using an explicit leapfrog scheme, and (2) is solved using a modified version of a steady state transport code [*Lummerzheim*, 1987]. A cross-section set [*Lummerzheim and Lilensten*, 1994] is used for the cross sections of molecular nitrogen, oxygen, and atomic oxygen. Mass Spectrometer Incoherent Scatter 90 (MSIS-90) [*Hedin*, 1991] is used to provide the neutral atmospheric densities, and International Reference Ionosphere 93 (IRI93) [*Bilitza et al.*, 1993] is used to obtain the ambient electron densities.

3. Comparisons With Steady State Calculations

In order to determine the limitations imposed by our assumptions, we use the steady state solutions to the transport equation from *Lummerzheim and Lilensten* [1994] as a standard to which we will compare. This steady state model has been tested against other transport calculations [*Strickland et al.*, 1989; *Solomon*, 1993] and agrees within 10%, the uncertainty in the different cross-section sets. We examined the effects of including the elastic cross sections versus turning off the elastic cross sections in the steady state equation. From understanding these effects, we have changed the loss function in (1) to simulate the effect of scattering on the transport of precipitating electrons.

We calculated the steady state ionization rate for two beams of electrons represented by Gaussian functions in energy with characteristic energies of 700 eV and 2.2 keV with half-widths 10% of their characteristic energy and all with a downward energy flux of 1 mW m^{-2}. For each beam we obtained two ionization rate profiles: one in which scattering was included in the transport calculation and one in which the scattering was turned off. In Figure 1 we show the resulting ionization rates for such calculations. As this figure shows, the altitude of the peak ionization rate can be significantly lower in height and larger in magnitude for the case without scattering than for the case with scattering. For the 700 eV beam, the peak ionization rate is $\sim$ 20 km lower in height and 33% larger in magnitude, and for the 2.2 keV beam the peak is $\sim$ 10 km lower and 56% larger.

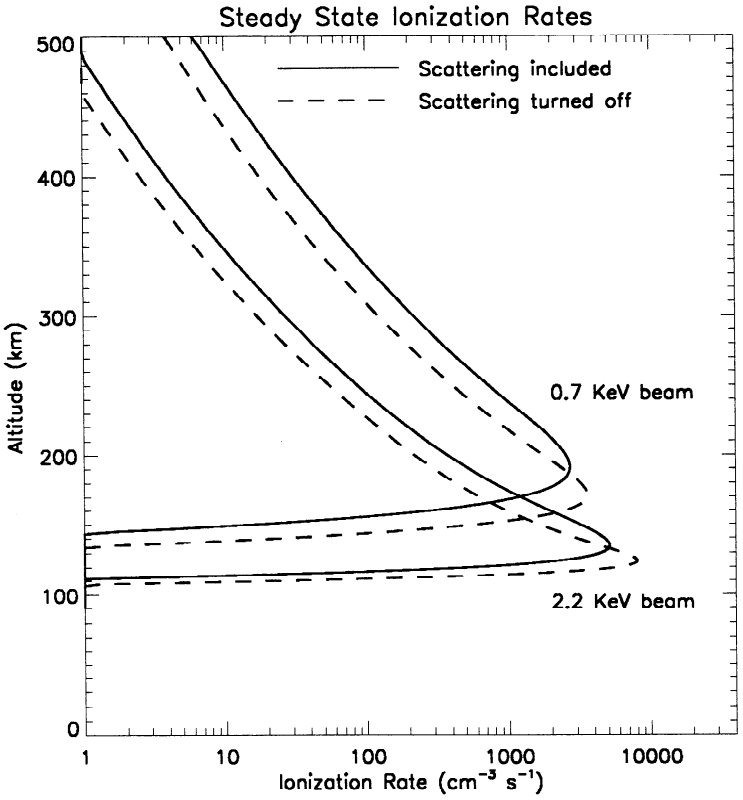

Figure 1. Ionization rates for two beams of electrons with characteristic energies of 700 eV and 2.2 keV. These ionization rate profiles were calculated by a steady state transport model with and without scattering included. The solid line indicates the solution with scattering and the dashed line shows the solution with scattering turned off.

When scattering is included, monodirectional electron distributions will isotropize. This lengthens their paths, which are spiral trajectories, in the atmosphere. And since an electron with a longer path length has a higher probability of colliding with an atmospheric neutral at a given height, scattered electrons lose energy at higher altitudes than electrons which do not scatter.

To compare our time-dependent calculations to the steady state solution, we run our model until there is no significant change in the ionization rate in time. We use a monoenergetic, field-aligned beam of electrons modeled by a Gaussian function in energy. The first comparison case has a peak energy of 700 eV, a half-width of 98 eV and a downward energy flux of 1 mW m^{-2}, and the second case has a peak energy of 2.2 keV, a half-width of 220 eV, and a downward energy flux of 1 mW m^{-2}. Both the steady state and the time-dependent calculations use the same MSIS-90 atmosphere and the same cross-section set.

The time required to reach steady state depends on the incident energy. Both beams were started at an altitude of 630 km at t=0 s. Below 300 km the ionization rate shown in Figure 2 stopped changing after 0.152 s for the 2.2 keV beam and for the 700 eV beam, it stopped changing after 0.108 s. The ionization rate above 300 km was still increasing at the end of the two runs after 0.330 seconds. This gives an indication of the timescales involved for auroral electron intensities to come to a steady state in phase space. An important factor is the timescale associated with low-energy secondary electrons. Because the collision frequency is lower at higher altitudes (due to the lower neutral and plasma densities), the production of low-energy secondary electrons at high altitudes is less. The intensity of these electrons will continue to increase until the rate of production of secondary electrons is equal to the rate of loss of these electrons to the thermal electron population. This process occurs much faster (less than a few milliseconds) below 150 km than above 150 km. The timescales of the order of 100 ms to obtain a steady state are due to the timescales above 150 km.

Figure 2 shows the steady state ionization rate with the time-dependent ionization rate after reaching steady state below 300 km. To obtain such good agreement in the altitude of the peak ionization rate, we had to multiply the loss function in (1) by a factor of 2 to simulate the longer path length that scattering implies. We calculated the difference between the two models at each altitude grid point. At the peak ionization rate, the difference in the calculations is 20% in the 700 eV beam and 5% in the 2.2 keV beam. The column integrated ionization rate, which is proportional to the

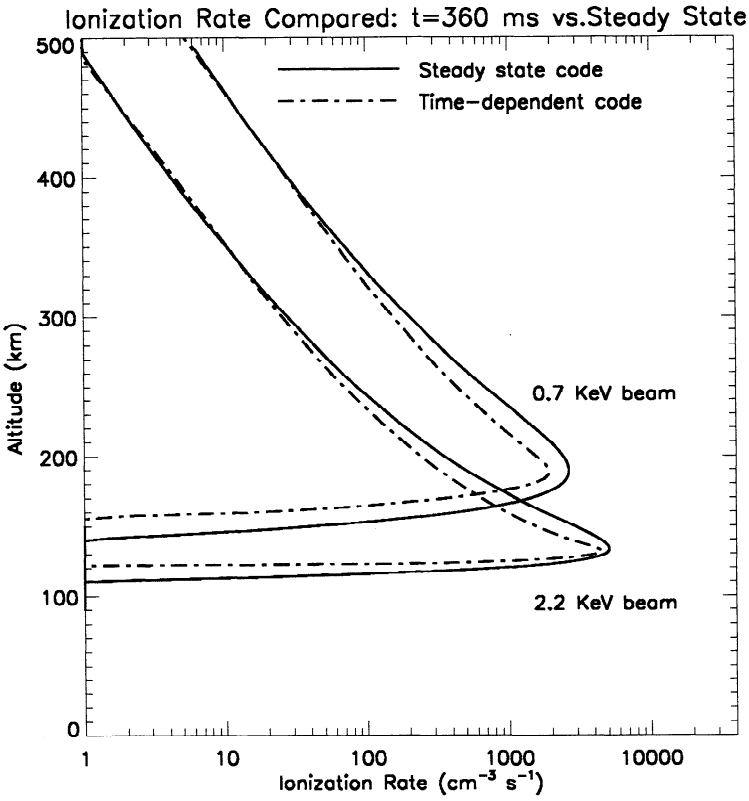

Figure 2. The comparison of a steady state transport calculation and the time-dependent calculation after 0.33 s when the ionization rate has reached its maximum. The steady state ionization rate as a function of altitude is shown in solid lines, and the dashed line represents the time-dependent ionization rate.

emission rate we use later in the paper, is $\sim$ 39% less for the time-dependent calculation than for the steady state calculation. The large differences of 40% in the altitude dependent ionization rate occur just above the peak ionization rate where scattering would fill in the ionization rate. This effect has not been compensated for by increasing the loss function.

It is important to note that the CSD assumption, which is not valid at energies below 3 keV, also leads to errors in the calculation at altitudes higher than the peak ionization rate. Instead of an integral collision term in which a fraction of the intensity moves to lower energy at all energies due to probabilities of colliding and losing different amounts of energy, the derivative collision term acts to continuously lose energy at a specific rate. At high energies the difference is not large because the fraction of energy lost in a collision compared with the energy of the beam is low, but with a lower energy beam where the collision cross sections are high, the fraction of energy lost is large. Not only will there not be enough electrons at higher altitudes and energies just below the beam energy, but since the beam does not lose enough energy at the high altitudes, it will deposit the bulk of its energy too low in the atmosphere.

The best course of action would be to include the scattering integral, increase the energy grid to higher energies, calculate discrete energy losses instead of using the CSD approximation, and combine (1) and (2) in a single equation. However, the time-dependent equation cannot be solved with these improvements with the present computational resources available to us. We can, however, provide some insight and guidance to flickering aurora studies and field-aligned bursts of electrons with our model as it stands.

4. Field-Aligned Bursts of Electrons

Arnoldy et al. [1999] have shown with the PHAZE II rocket data that FABs responsible for flickering aurora often show a 100% on-off modulation of the down going flux. They, as well as others [*Spiger and Anderson*, 1985; *McFadden et al.*, 1987], have demonstrated that these FABs have significant flux from the peak electron flux energy down to energies lower than 50 eV. For this study, we assume the source intensities to be field-aligned and constant in energy up to the highest energy on our energy grid, 3.0 keV, and with a total flux of 1 mW m^{-2}. This intensity is assumed to be turned completely on and off at an altitude of 4000 km. We

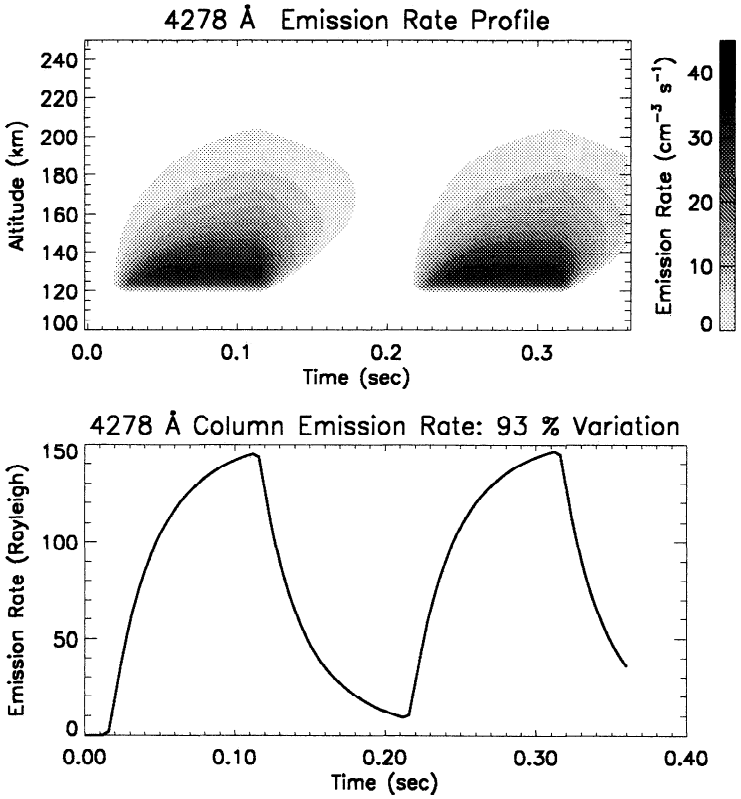

Figure 3. The effect on optical emissions of field-aligned beams modulated at 5 Hz from 4000 km. (top) The altitude dependent 4278 Å emission rates over time due to the FABs. (bottom) The column integrated emission rates.

then perform a collisionless velocity dispersion calculation to get the intensity at the top of the simulation box at 600 km altitude as a function of time. This study is not concerned with the mechanisms which create flickering but the observable optical effect of flickering in the ionosphere.

For this study, we use two typically seen flux modulation frequencies, as mentioned in the above references, of 5 and 100 Hz. For the optical emission, we model the prompt $N_2^+(1NG)$ (4278 Å) emission. We do this because it is directly proportional to the ionization rate and gives the best indication of the quick response of the ionosphere. The green 5577 Å emission has a long lifetime (0.7 s). Because of this lifetime, it acts as a DC offset in optical emissions on the timescales we are discussing in this paper. The same applies to the red OI 6300 Å emission which has a lifetime of 110 seconds. When making white light observations these emissions and others must be taken into account.

The results of this study are shown in Figure 3 for the 5 IIz case and Figure 4 for the 100 Hz case. Figures 3(top) and 4(top) are the 4278 Å emission rate as a function of altitude and time. Figures 3(bottom) and 4(bottom) show the altitude integrated emission rate to show what a filtered photometer looking in the zenith at the flickering aurora would observe. The $N_2^+(1NG)$ emission is prompt, which allows us to resolve the effect of such rapidly varying precipitating fluxes on the ionosphere. We calculate the percent difference between the peak and the valley of the column integrated emission rate to obtain the maximum variation in column emission rates. We find that for the 5 Hz electron modulation there is a 93% difference between the peak and the valley of the emission rate. For the 100 Hz modulation the variation drops to 12%.

The remaining "afterglow" emission rate in Figures 3 and 4 after the precipitating electrons have been turned off is primarily due to the velocity dispersion in the electrons. It is this effect of the dispersion which smoothes the optical column emission rate because the low-energy electrons penetrate into the ionosphere after the down going electron flux has been turned off. These electrons deposit their energy higher in altitude than the high energy electrons which reach the ionosphere first. There is also a small effect due to the slowly decaying secondary electron intensity which is dependent on the loss of energy to the neutral atmosphere and thermal electron population (L_{ee} in equation (2)). The secondary electron intensity decay is less than a few milliseconds below 150 km, but at higher altitudes this decay can take up to 100 ms. However, the emission rate, already low at altitudes above 150 km, decreases quickly in the first 10 ms and so is only important for very high frequencies of flux modulations.

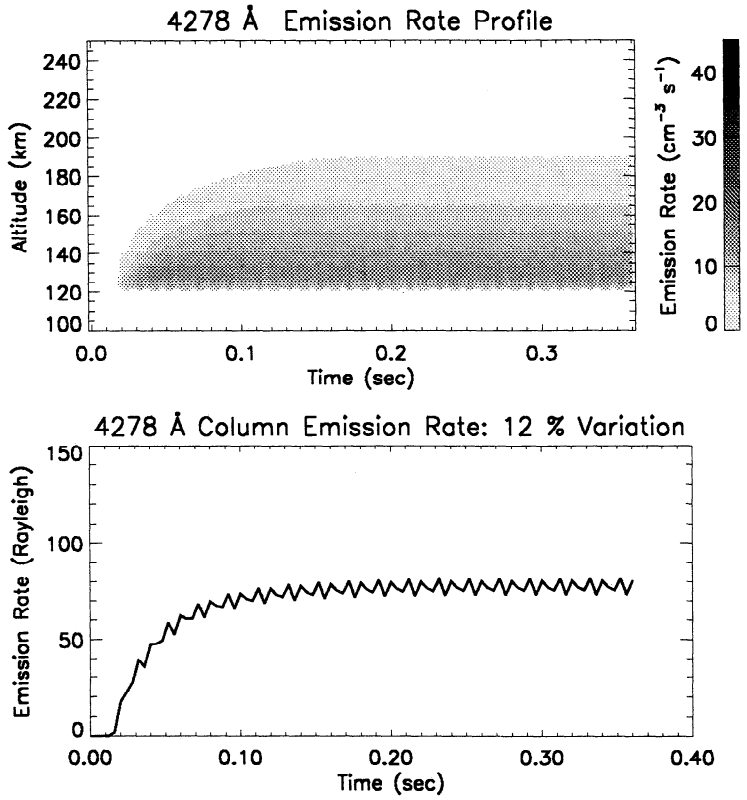

Figure 4. Same as Figure 3, but for a 100 Hz modulated signal.

Figures 3 and 4 are quite different in their column brightness. This height integrated emission rate of the $N_2^+(1NG)$ in flickering aurora peaks lower for the higher frequency case, although the incident electron flux is the same as in the low-frequency case (1 mW m^{-2}). This is due to the time averaging that occurs from the dispersive transport of precipitating electrons. Averaging the brightness over many on-off pulses yields the same brightness in both cases and is in agreement with the brightness of the steady state model when driven with the time-averaged precipitation (i.e., with a constant energy flux of 0.5 mW m^{-2}). Even though the emission is prompt, the temporal variation of the electron intensity in the ionosphere gives it the appearance of an emission from a long lived state.

The solution to the transport equation for flickering aurora gives us the electron intensity as a function of time, energy, and altitude. It is possible, then, to look at the results from the perspective of a rocket flying through such FABs. Shown in Figure 5 and in Figure 6 is the field-aligned, downward electron flux as a function of time at 502 km and at 153 km, repectively, as the 5 Hz modulated FABs propagate along the field line. In order to demonstrate what this might look like to an electron detector flying at the two altitudes at an instant in time, we have taken a slice of each flux at 348 ms, converted it to distribution function and plotted it below the time-dependent spectra.

In the flux of Figure 5 one can clearly see the dispersion of the primary energy spectra as these two beams reach 502 km. This dispersion is very similar to that seen in the fluxes shown by *Arnoldy et al.* [1999], especially in their Figure 2 and Plate 4. It is important to note that the low-energy secondary electrons in Figure 5 are exaggerated due to the assumption that they do not travel downward. At this altitude, the atmospheric density is low enough that the probability of collisions is small, and the electrons which are created from ionization collisions should transport away from this region.

The bumps shown in the distribution function of Figure 5 are due to the two FABs: one which has recently been turned on and only the high energy electrons have arrived at the altitude of the rocket and a second one which has been turned off for a while and only the low-energy electrons are still propagating into the ionosphere. The plateau represents the original flat intensity which was assumed as the upper boundary condition. With higher frequency modulation of the down-going flux, there will be more bumps, and they will have shorter energy spans. If the time resolution of the instruments measuring the electron differential flux is not sufficient, the flux at different energies will overlap, resulting in a distribution function which is fairly constant over many energies.

Since the instruments used by *Arnoldy et al.* [1999] have high enough energy and time resolution to see the dispersion in the FABs, when this PHAZE II elec-

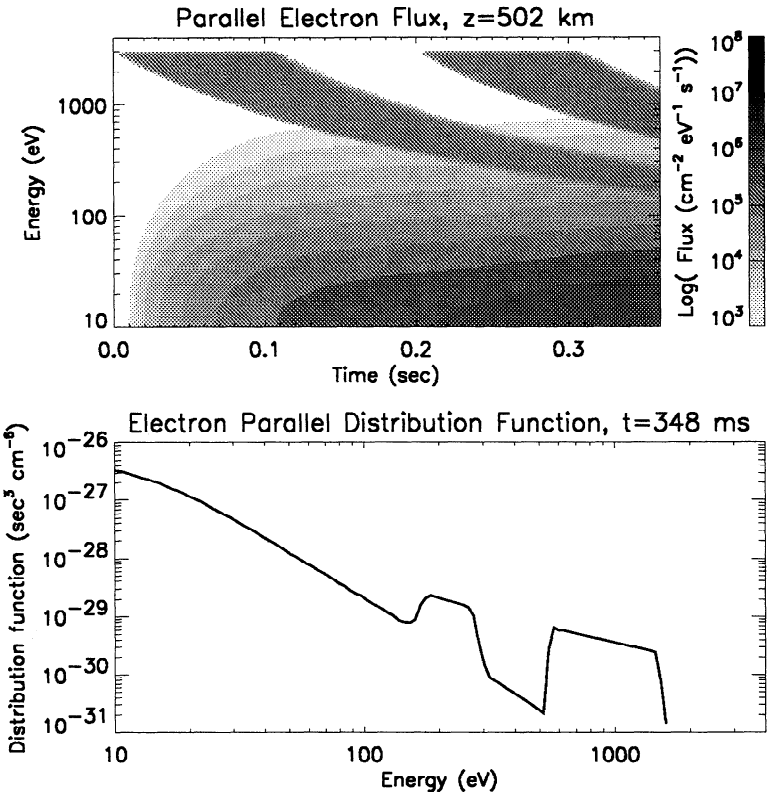

Figure 5. The differential electron flux as an instrument on a rocket or satellite might record it. (top) The field-aligned flux as a function of energy and time at 502 km altitude. (bottom) A cut at t=0.348 s of the Figure 5(top) which has then been converted to distribution function from flux.

tron data is plotted as a distribution function, multiple bumps are seen [*Semeter et al.*, 1999]. *McFadden et al.* [1990] also see similar bumps in field-aligned distribution functions measured by electron detectors on a sounding rocket during the Berkeley Ionospheric Dual Altitude Rocket Campaign. They explain these plateaus as due to waves created by the semi-unstable distribution function. From our results it seems more likely that the plateaus seen in these rocket electron distributions are simply due to measuring multiple FABs at a particular time and space in the aurora. If this interpretation is correct, it may be possible to deduce from rocket or satellite measurements not only the source altitude but also the source distribution function. The knowledge of the source distribution function should help to determine the process for generating modulated FABs detected during flickering aurora.

By comparing Figure 6 with Figure 5, it becomes clear how collisions affect the electrons at 150 km. As time passes the low-energy electrons of the pulse eventually reach this altitude, where they are slowed down and stopped much faster than at 500 km where they continue to move through the region at their original velocity. Figure 6 also shows how the distribution function, if sampled at a time when the pulse is still on, will look flat at high energies because of the large energy loss to the ionosphere. The effect of this energy loss is greater in denser atmosphere and at low energies where the electron-neutral collision cross sections are largest. The altitude above which neutral-electron collisions are negligible will also change with the solar cycle since the atmosphere expands during solar max and increases in density at higher altitudes during these years. This can also be true of very active aurora which heats the thermosphere.

5. Discussion

Our model, in spite of our approximations suggests some possible explanations to past conflicting data sets. *Evans* [1967] and *Spiger and Anderson* [1985] measured electrons less than a few keV as well as high-energy electrons greater than 10 keV. Strongest modulations in these data sets were detected in the higher-energy electrons, whereas in other data sets [*Lin and Hoffman*, 1979; *Arnoldy et al.*, 1985; *McFadden et al.*, 1987], strong modulations were detected in the lower-energy electron flux. The difference in these data sets is that the rockets flown by *Evans* [1967] and *Spiger and Anderson* [1985] were both below 190 km when flickering was observed, whereas the other rockets and satellites were above 200 km. As shown in Figure 6, as compared with Figure 5, electrons less than 2 keV lose energy below 150 km due to collisions with the ionosphere. It is

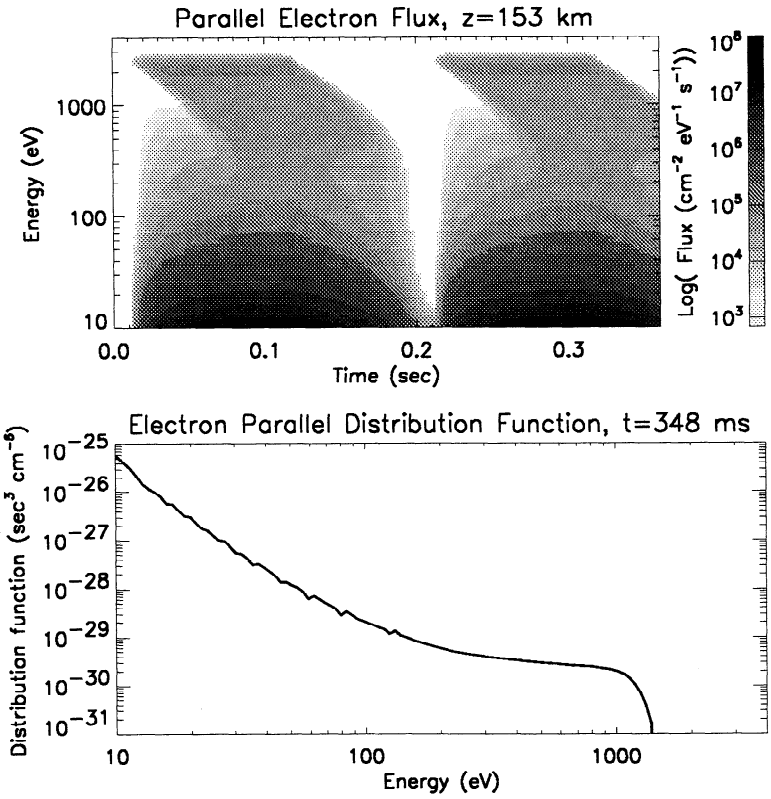

Figure 6. Same as in Figure 5, but for an observer at 153 km altitude.

feasible then that the lower-energy electrons measured by *Evans* [1967] and *Spiger and Anderson* [1985] were modified by the upper atmosphere and the modulations in these energies were not detected. The high-energy electrons have a smaller probability of colliding due to the energy dependent cross sections and thus would not be affected by the atmosphere at the altitudes through which the instruments flew.

It is also important to consider at what altitude the in-situ measurements of electron fluxes are taken if the velocity dispersion of these fluxes is used to obtain the acceleration region altitude. As shown in Figure 6, the loss of energy to the atmosphere is large. If we were to assume no atmospheric loss and calculate a source altitude for this beam from the apparent dispersion, we obtain as the source altitude 2000 km instead of the actual 4000 km we used in this simulation. As mentioned above, the effect of the atmosphere depends strongly on the energy of the electrons and the atmospheric density. *Evans* [1967] calculates a source altitude of no more than 1300 km from in-situ electron flux modulations using dispersion calculations while the rocket is flying between 90 and 150 km. While the electrons detected below 16 keV will probably give source regions which are too low due to the loss of energy to the atmosphere at the detection altitudes, the 60 and 120 keV electrons should still give an accurate source calculation assuming velocity dispersion between these electrons. We therefore conclude that the source altitude of the modulations in electron flux in the tens to hundreds of keVs that *Evans* [1967] calculated is correct. There are a few explanations for electron flux modulation in the ionosphere below 1500 km [*Evans*, 1967; *Perkins*, 1968; *Lin and Hoffman*, 1979; *McHarg et al.*, 1998] as well as explanations for the modulation occurring at higher altitudes between 2500 and 8000 km [*Temerin et al.*, 1986, 1993; *Arnoldy et al.*, 1999]. Our study on field-aligned bursts assumes the source region is found at 4000 km and the agreement between Figure 5 and *Arnoldy et al.* [1999] and *McFadden et al.* [1987] strongly suggests that the main electron modulations which create flickering aurora occurs near the acceleration region, which is found at these high altitudes. However, it may be, as *McHarg et al.* [1998] suggest, that there is more than one process acting to modulate precipitating electrons.

With a time-dependent transport code and recently developed instruments, such as the high speed imager at the University of Alaska, Fairbanks, which has a frame rate of 1000 frames/second (H. Stenbaek-Nielsen, personal communication, 1999) or a 16 channel high speed photometer such as the one used by *McHarg et. al* [1998], we should be able to deduce an upper bound on the altitude at which the electrons creating a flickering auroral display are modulated. Such instruments are well suited to detect the integrated column intensity variation in flickering aurora. It is possible to study more closely the variation of the column inte-

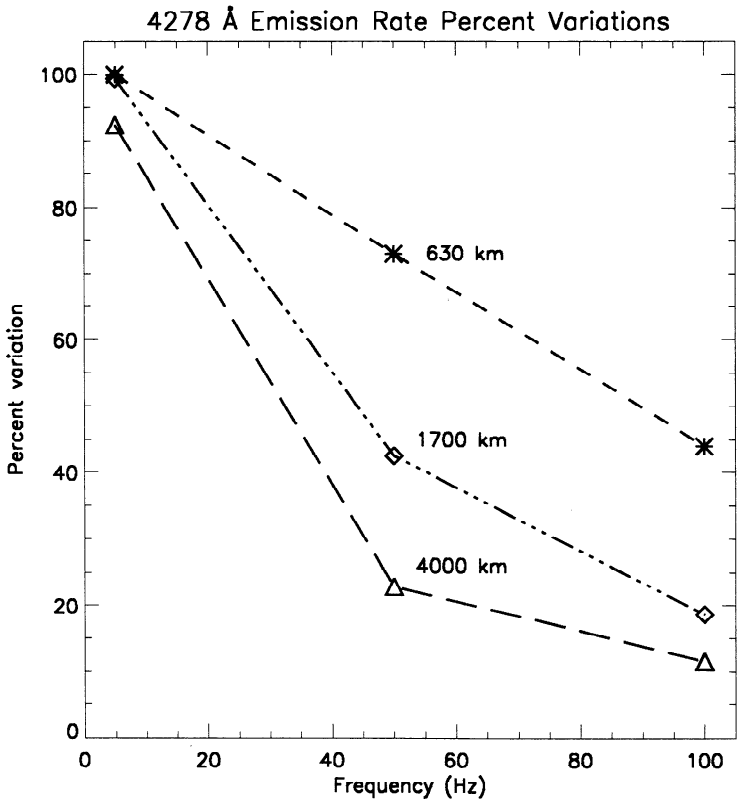

Figure 7. The variation in optical emission of 4278 Å as a function of frequency for three different source altitudes using the same initial downward electron intensities as for Figures 3 and 4.

grated 4278 Å emission rate with our model and relate our results to the height at which the electrons are modulated.

To demonstrate what type of study one could do with a more complete time-dependent transport code, we ran the time-dependent simulation for three different source altitudes and three different frequencies. The results are shown in Figure 7 which shows the brightness modulation of the height integrated emission rate as a function of frequency for different source altitudes. The higher the frequency, the less the variation in brightness due to the velocity dispersion in the electrons and the slow decay of the higher altitude secondary intensities. The closer the source is to the atmosphere, the greater the variation since there is less dispersion. Given integrated optical column intensity variations of 4278 Å of suprathermal field-aligned electron bursts, Figure 7 provides an upper bound on the altitude from which the bursts come.

Measurements have recently been taken using an array of filtered photometers during flickering aurora [*Sakanoi and Fukunishi*, 1999]. *McHarg et al.* [1998] have made high speed photometer measurements of flickering aurora with white light. In order to use such observations of brightness variations in flickering aurora with the transport calculation results, as in Figure 7, it is necessary to address some remaining issues. For white light measurements, it is important to include with the time-dependent transport calculation a synthetic spectrum to simulate white light measurements. It is also important to note that most of the electron fluxes which cause flickering aurora are not only low energy, cold, field-aligned bursts but also high energy, hot, pitch angle dispersed electrons as discussed in references above. This part of the spectra must be included in the model to obtain correct percent variation in optical brightness. Since the inverted-V electrons are often greater than 3 keV, these electrons will deposit their energy lower in the atmosphere and will create larger variations in brightness. However, these electrons are also pitch angle dispersed, which will smooth the optical signal since electrons at larger pitch angles will deposit their energy at a later time than the field-aligned inverted-V electrons as well as at an altitude higher than these field-aligned electrons. Taking into account these considerations, it should be possible to use ground based optical measurements recording flickering aurora and a time-dependent transport code to obtain an upper bound on the modulation source altitude.

6. Summary

We have developed a time-dependent auroral electron transport model. In order to overcome numerical difficulties that result in unrealistic computer requirements, we have introduced a number of compromises:

The energy loss of the high energy electrons is treated as a continuous slowing down process; high energy electrons experience only forward scattering; low-energy (secondary) electrons have discrete energy losses but no transport in altitude. Comparison with a steady state solution to the Boltzmann equation shows that these assumptions lead to different altitude profiles of the ionization rates which can be largely corrected by a modified loss function. Our numerical experiments show that future time-dependent transport calculations should include discrete energy losses and scattering for energetic electrons with energy less than 3 keV. Scattering is important in energy deposition studies largely because it will isotropize electron intensities and the average path length of the electrons will increase, thus increasing the probability of electrons colliding and losing energy to excitation and ionization of neutral atoms and molecules. This energy loss is a discrete process and must be included as such for auroral electrons.

We used our model to study field-aligned bursts in flickering aurora. For a constant downward flux to propagate from 600 km to the lower ionosphere and to come to a steady state configuration it takes $\sim$ 100 ms, which shows that it is necessary to use a time-dependent calculation to study emission rates of flickering aurora modulated at frequencies greater than 5 Hz. By comparing a 100 Hz versus a 5 Hz electron modulation, we are reminded that it is the time-averaged downward flux which gives the correct time-averaged emission rate. Of the physics included in the transport calculation, velocity dispersion of the modulated downward precipitating electrons is the most important process which affects the 4278 Å emission rate modulation. The effect of this dispersion is different depending on the altitude where the field-aligned electron beams are modulated. From this, it seems possible to determine an upper bound on the altitude of the electron source.

Rocket and satellite differential flux measurements are common and important in studying flickering aurora and FABs. We have shown that velocity dispersion calculations need to be done well above 150 km for electrons less than $\sim$ 2 keV because the energy degradation of these electrons in the upper atmosphere obscures the velocity dispersion. From the similarity of the differential flux at 502 km of this study to that of the data by *Arnoldy et al.* [1999] and *McFadden et al.* [1987], there must be flickering aurora which is a result of electrons modulated at altitudes well above the lower ionosphere. These similarities also agree with the interpretation that the bursts seen in rocket and satellite detectors are a temporal rather than a spatial phenomena. With sufficient time resolution, one should be able to reconstruct the initial electron intensity from the bumps in the distribution function. We cannot rule out the possibility of modulations in the lower ionosphere our study, though we can explain the discrepancy between the in-situ modulation of high-energy electron versus low-energy electron modulations.

Acknowledgments. We would like to thank Hans Stenbaek-Nielsen, Tom Hallinan and Geoff McHarg for inspiring discussions regarding flickering aurora, Antonius Otto for guidance with numerical techniques and the NASA Graduate Student Researchers Program for funding this research under grant number NGT5-50191. We also thank the referees for helpful comments that have improved our paper.

Janet G. Luhmann thanks Michael W. Liemohn and Eric J. Lund for their assistance in evaluating this paper.

References

Arnoldy, R. L., Rapid fluctuations of energetic auroral particles, *J. Geophys. Res.*, *75*, 228, 1970.

Arnoldy, R. L., T. E. Moore, and L. J. Cahill Jr., Low-altitude field-aligned electrons, *J. Geophys. Res.*, *90*, 8445, 1985.

Arnoldy, R. L., K. A. Lynch, J. B. Austin, and P.M. Kintner, Energy and pitch angle dispersed auroral electrons suggesting a time-variable inverted-V potential structure, *J. Geophys. Res.*, *104*, 22,613, 1999.

Banks, P. M., and A. F. Nagy, A new model for the interaction of auroral electrons with the atmosphere: Spectral degradation, backscatter, optical emission, and ionization, *J. Geophys. Res.*, *79*, 1459, 1974.

Beach, R., G. R. Cresswell, T. N. Davis, T. J. Hallinan, and L. R. Sweet, Flickering, a 10 cps fluctuation within bright auroras, *Planet. Space Sci.*, *16*, 1525, 1968.

Berkey, F. T., M. B. Silevitch, and N. R. Parsons, Time sequence analysis of flickering auroras, 1, Application of fourier analysis, *J. Geophys. Res.*, *85*, 6827, 1980.

Bilitza, D., K. Rawer, L. Bossy, and T. Gulyaeva, International reference ionosphere - Past, present, future, *Adv. Space Res.*, *13*, 3, 1993.

Evans, D. S., A 10-cps periodicity in the precipitation of auroral-zone electrons, *J. Geophys. Res*, *72*, 4281, 1967.

Hedin, A. E., Extension of the MSIS thermosphere model into the middle and lower atmosphere, *J. Geophys. Res.*, *96*, 1159, 1991.

Johnstone, A. D., and J. D. Winningham, Satellite observations of suprathermal electron bursts, *J. Geophys. Res.*, *87*, 2321, 1982.

Kunitake, M., and T. Oguti, Spatial-temporal characteristics of flickering spots in flickering auroras, *J. Geomagn. Geoelectr.*, *36*, 121, 1984.

Lin, C. S., and R. A. Hoffman, Fluctions of inverted-V electron fluxes, *J. Geophys. Res*, *84*, 6547, 1979.

Lummerzheim, D., Electron transport and optical emissions in the aurora, Ph.D. thesis, Univ. of Alaska, Fairbanks, 1987.

Lummerzheim, D., and J. Lilensten, Electron transport and energy degradation in the ionosphere: Evaluation of the numerical solution, comparison with laboratory experiments and auroral observations, *Ann. Geophys.*, *12*, 1039, 1994.

Lund, E. J. et al., Observation of electromagnetic oxygen cyclotron waves in a flickering aurora, *Geophys. Res. Lett.*, *22*, 2465, 1995.

McFadden, J. P., C. W. Carlson, M. H. Boehm, and T. J. Hallinan, Field-aligned electron flux oscillations that produce flickering aurora, *J. Geophys. Res.*, *92*, 11,133, 1987.

McHarg, M. G., D. L. Hampton, and H. C. Stenbaek-Nielsen, Fast photometry of flickering in discrete auroral arcs, *Geophys. Res. Lett.*, *25*, 2637, 1998.

Opal, C. B., W. K. Peterson, and E. Beaty, Measurements of secondary-electron spectra produced by electron impact ionization of a number of simple gases, *J. Chem. Phys.*, *55*, 4100, 1971.

Perkins, F. W., Plasma-wave instabilities in the ionosphere over the aurora, *J. Geophys. Res.*, *73*, 6631, 1968.

Sakanoi, K. and H. Fukunishi, Multi-anode fast photometer observations of flickering aurora at Syowa Station, *Eos Trans. AGU*, *80*(46), Fall Meet. Suppl., F767, 1999.

Semeter, J., D. Lummerzheim, R. L. Arnoldy, K. A. Lynch, J. Vogt, and G. Haerendel, Modeling optical emissions of flickering aurora, *Eos Trans. AGU*, *80*(17), Spring Meet. Suppl., S250, 1999.

Solomon, S. C., Auroral transport using the Monte Carlo method, *Geophys. Res. Lett.*, *20*, 185, 1993.

Spiger, R. J., and H. R. Anderson, Fluctuations of precipitated electron intensity in flickering auroral arcs, *J. Geophys. Res.*, *90*, 6647, 1985.

Stamnes, K., On the two-stream approach to electron transport and thermalization, *J. Geophys. Res.*, *86*, 2405, 1981.

Strickland, D. J., D. L. Brook, T. P. Coffey, and J. A. Fedder, Transport equation techniques for the deposition of auroral electrons, *J. Geophys. Res.*, *81*, 2755, 1976.

Strickland, D. J., R. R. Meier, J. H. Hecht, and A. B. Christensen, Deducing composition and incident electron spectra from ground based auroral optical measurements: Theory and model results, *J. Geophys. Res.*, *94*, 13,527, 1989.

Temerin, M., J. McFadden, M. Boehm, and C. W. Carlson, Production of flickering aurora and field-aligned electron flux by electromagnetic ion cyclotron waves, *J. Geophys. Res*, *91*, 5769, 1986.

Temerin, M., C. Carlson, and J. P. McFadden, The acceleration of electrons by electromagnetic ion cyclotron waves, in *Auroral Plasma Dynamics*, Geophys. Monogr. Ser., vol. 80, edited by R. Lysak, pp. 155, AGU, Washington, D.C., 1993.

D. Lummerzheim and L. Peticolas, Geophysical Institute, University of Alaska Fairbanks, 903 Koyukuk Dr, P.O. Box 757320, Fairbanks, AK 99775. (LMP@gi.alaska.edu)

(Received October 28, 1999; revised January 18, 2000; accepted January 19, 2000.)